

## GRAPHENE/ $Zn_xCdS$ NANOPATES FOR ENHANCED PHOTOCATALYTIC PROPERTIES

B. ZENG\*, W. ZENG

*College of Mechanical Engineering, Hunan University of Arts and Science, Changde 415000, People's Republic of China*

A novel graphene/ $Zn_xCdS$  nanoplates solid solution (G/ $Zn_xCdS$  NP) had been successfully synthesized via microwave method and showed their excellent photocatalytic activity. The nanocomposites with different atomic ratios of Zn/Cd were synthesized and their corresponding photocatalytic performance was examined. The synergistic effect of enhanced photocatalytic activity revealed the presence of  $Zn_xCdS$  nanoplates solid solution, having a preferable narrow band gap with strong redox ability and effective charge separation along with graphene in the composites. The present research provides an effective method for the development of photocatalysts which will be beneficial to solve the environmental pollution.

(Received February 17, 2019; Accepted July 29, 2019)

*Keywords:* Graphene, Solid solution, Photocatalytic

### 1. Introduction

Photocatalytic technology is a promising method for solving the problems related to the environmental pollution[1]. Different types of photocatalysts, such as metal oxides, metal sulfide and nitride semiconductors have been investigated so far[2-3]. Among them, CdS has proved to be highly efficient as a visible photocatalyst because of its narrow band gap ( $E_g = 2.4$  eV). However, the low conduction band (CB) location leads to a weak redox ability of photogenerated electrons in photocatalytic reaction[4]. Compared with CdS, the CB edges of ZnS are located to the more negative region which led to enhanced redox ability of photogenerated electrons due to the presence of large number of reductive photoexcited electrons[5]. Therefore, by coupling ZnS and CdS to form  $Zn_xCdS$  solid solution will have more powerful impact on redox capability, resulting excellent photocatalytic activities[6]. Furthermore, by controlling the atomic ratio of Zn/Cd, the  $Zn_xCdS$  solid solution exhibits widely tunable band gaps which can adjust absorption response in the visible light region, thus favoring the photocatalytic activity[7].

Due to large surface areas, excellent optical properties and unique electronic behavior in different confined dimensions, two-dimensional (2D) nanostructure has served an excellent photocatalytic performance, as shown in previous studies[8-9]. Thus, it is reasonable to achieve high-efficiency photocatalysts by using 2D  $Zn_xCdS$  solid solution.

In addition, the rapid photogenerated electron-hole recombination in the nanocomposites

---

\* Corresponding author: 21467855@qq.com

seriously obstructs their photocatalytic activity[10]. Graphene with high electronic conductivity can function as an electron transporter to accommodate the photogenerated electrons, thereby developing novel graphene/ZnxCdS nanocomposites to enhance the photocatalytic performance[11]. However, the integration of 2D ZnxCdS solid solution and graphene has never been reported.

Considering all the aforementioned issues together, we herein developed a graphene/ZnxCdS nanoplates solid solution (G/ZnxCdS NP) via microwave method. The experimental results revealed that the photocatalytic efficiency of this nanomaterial was significantly enhanced.

## 2. Experimental details

### 2.1. Preparation of G/Zn<sub>x</sub>CdS NP

In the typical preparation, proportioned (50:50 by volume) of ethylene glycol (C<sub>2</sub>H<sub>6</sub>O<sub>2</sub>, ≥ 99.9% purity, Aladdin) and 50% of deionized water were adequately mixed. Then, optimal graphene oxide (GO) (0.01 g) was added and stirred thoroughly for 10 min. 0.6 g of Cd(Ac)<sub>2</sub>·2H<sub>2</sub>O and a certain amount of Zn(Ac)<sub>2</sub>·2H<sub>2</sub>O were dissolved completely into the above solution. Consequently, 0.5 g of thiourea (H<sub>2</sub>NCSNH<sub>2</sub>, ≥ 99.0% purity, Aladdin) was added into it. The entire reaction mixture was then heated in a microwave power for about 60 min under continuous stirring. Finally, the as-products were washed several times with deionized water and dried in a vacuum oven at 60 °C for 12 h. The atomic ratio of Zn/Cd in precursors was 0:1, 0.2:1, 0.4:1, 0.6:1, and the resulting samples were labeled as G/Zn<sub>0</sub>CdS NP, G/Zn<sub>0.2</sub>CdS NP, G/Zn<sub>0.4</sub>CdS NP, and G/Zn<sub>0.6</sub>CdS NP, respectively.

### 2.2. Characterization

The phase and structure of the product were confirmed by X-ray diffraction (D5000, Siemens, Germany) by using Cu K $\alpha$  radiation. The optical properties were tested by spectrophotometry (UV-2500, Shimadzu, Japan). The functional groups presented in the nanocomposites were characterized by Fourier transform infrared spectrometer (WQF-410, Beijing Second Optical Instrument Factory, China). Ultraviolet-visible (UV-vis) absorption spectra were achieved by using a spectrophotometer (UV-2500, Shimadzu, Japan). The chemical state of the elements was identified by X-ray photoelectron spectroscopy (K-Alpha 1063, Thermo Fisher Scientific, USA). The morphology of the samples was characterized by both scanning electron microscopy (SEM, S4800) and transmission electron microscopy (TEM, JEM-2100F). The elemental analysis was conducted by energy-dispersive spectroscopy (EDS) in the TEM.

### 2.3. Photocatalytic experiment

The photocatalytic performance of G/Zn<sub>x</sub>CdS NP was evaluated by monitoring the photodegradation of methyl orange (MO). A typical experiment was involved by adding 20 mg of photocatalysts to 300 mL of MO solution (20 mg L<sup>-1</sup>) in the vessel. The suspension was magnetically stirred thoroughly for 30 min in darkness to establish the adsorption-desorption equilibrium and then exposed to irradiation by a 500 W xenon arc lamp. In every 10 min intervals of irradiation, 2 mL of reaction solution were collected and centrifuged to separate the

photocatalyst particles. The UV-visible absorption spectra of the supernate were acquired to determine the degradation efficiency of MO by recording the corresponding absorbance of the characteristic peak at 464 nm.

### 3. Results and discussion

The XRD patterns for G/Zn0CdS NP and G/Zn0.4CdS NP hybrid materials are shown in Fig. 1 a. G/Zn0CdS NP, namely G/CdS NP displayed the diffraction peaks located at 25.1°, 26.4°, 43.7°, 48.1°, and 51.7°, which were indexed to the crystal planes of CdS hexagonal phase (JCPDS No. 65-3414) as (100), (002), (110), (103) and (112), respectively.

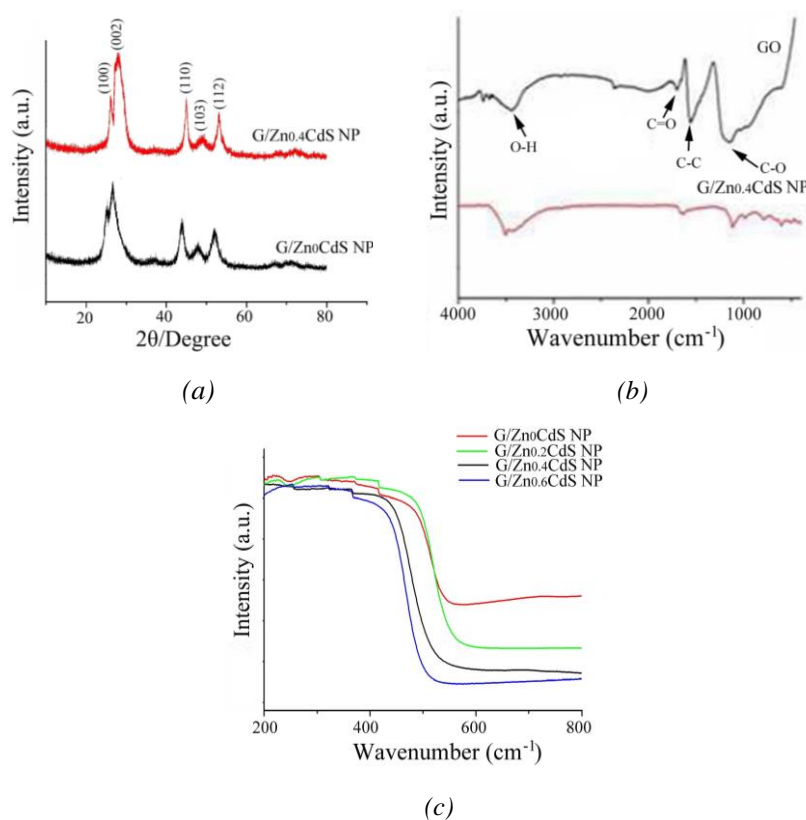


Fig. 1. (a) XRD spectra (b) FTIR spectra, (c) UV/Vis diffuse reflectance spectra of the samples.

Although the diffraction peaks of the sample, G/Zn0.4CdS NP was similar to Zn0CdS/G, but the shift towards the side of larger angles indicated that the hexagonal CdS structure was retained and a small amount of Zn<sup>2+</sup> ions could be incorporated into the lattice of CdS, confirming the formation of Zn<sub>0.4</sub>CdS solid solution[12]. In addition, no significant peaks of graphite were noticed in the spectra as there was a relatively low amount of graphene in the composites[13].

Fig. 1 b presents the FTIR spectra of GO (graphene oxide) and G/Zn0.4CdS NP. The characteristic peaks associated with C-O stretching (1084 cm<sup>-1</sup>), C-C stretching (1610 cm<sup>-1</sup>), C=O stretching (1713 cm<sup>-1</sup>) and O-H stretching (3444 cm<sup>-1</sup>) for GO are clearly seen in the spectra. In the G/Zn0.4CdS NP sample, all these bands were related to the functional groups, but those assigned to the oxygen-containing groups were either substantially reduced or even disappeared.

The results suggested that GO could be effectively transformed into graphene by the significant removal of oxygen-containing groups[14].

Fig. 1 c shows the UV-visible DRS spectra for G/Zn<sub>x</sub>CdS hybrid materials. A gradual blue shift of the absorption edge from 590 to 510 nm by increasing the Zn content has been observed. The band gap of G/Zn<sub>x</sub>CdS hybrid was adjusted by changing the atomic ratio of Zn/Cd. Besides, the high content of zinc in the G/Zn<sub>x</sub>CdS solid solution would limit the visible-light absorption and hence the incorporation of Zn<sup>2+</sup> ions into the CdS lattice can improve the redox capability. Therefore, by suitably adjusting the atomic ratio of Zn/Cd in the precursor, G/Zn<sub>x</sub>CdS NP will be endowed with the effective light response and excellent redox capability, thus favoring the photocatalytic reaction[15].

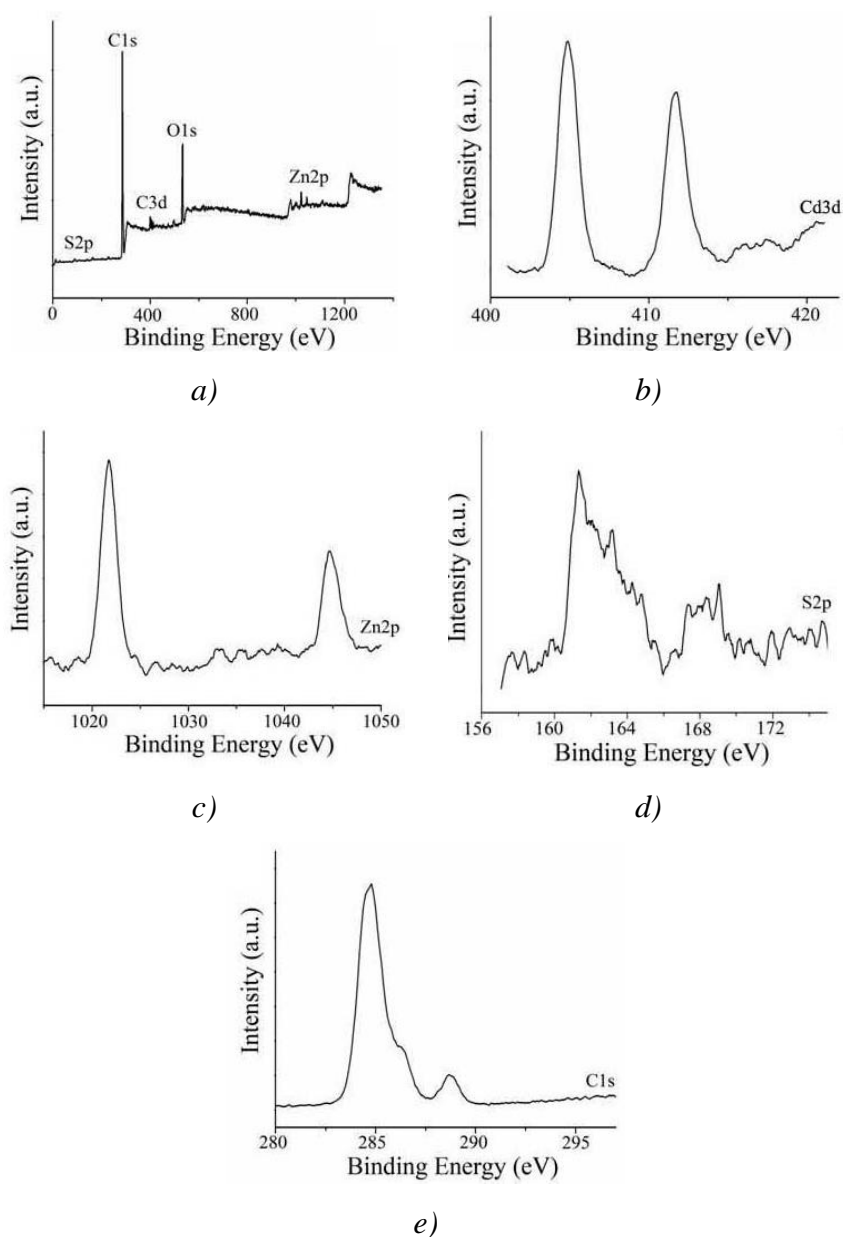


Fig. 2. Typical XPS spectra of the G/Zn<sub>0.4</sub>CdS NP composite: (a) Survey spectra, (b) Cd 3d region XPS spectrum, (c) S 2 p region XPS spectrum, (d) Zn 2 p region XPS spectrum, (e) C1s region XPS spectrum

Fig. 2 a depicts a wide scan XPS spectrum for G/Zn<sub>0.4</sub>CdS NP, and the signals received from cadmium, zinc, sulfur, carbon, and oxygen imply the formation of hybrid graphene/Zn<sub>x</sub>CdS solid solution. Fig. 2 b-e presents high-magnification XPS spectra in which the elemental composition of Zn 2p, Cd 3d, S 2p and C 1s for G/Zn<sub>0.4</sub>CdS are described. Among them, Cd 3d and Zn 2p spectra (Fig. 2b and c) demonstrate pairs of symmetrical and sharp peaks with binding energies of 404.8 eV (Cd 3d<sub>5/2</sub>), 411.7 eV (Cd 3d<sub>3/2</sub>), 1021.6 eV (Zn 2p<sub>3/2</sub>), and 1044.6 eV (Zn 2p<sub>2/1</sub>), respectively, indicating that Cd<sup>2+</sup> and Zn<sup>2+</sup> exist in the nanocomposites. Similarly, the presence of S 2p<sub>3/2</sub> peak at 161.3 eV and S 2p<sub>1/2</sub> at 163.2 eV (Fig. 2d) confirms that sulfur is in the state of S<sup>2-</sup>. All these peaks prove the existence of Zn-S and Cd-S bonds [16]. In addition, the C 1s spectra for G/Zn<sub>0.4</sub>CdS, centered at 284.8 eV is attributed to the C-C sp<sup>2</sup> bonding in the graphitic structure while we revealed a small amount of oxygen containing functional groups by fitting the peak at 288.6 eV. Besides, the presence of strong intensity of sp<sup>2</sup> indicates that an effective reduction of GO occurs in the nanocomposites which results in an effective charge separation [17]. Therefore, the weak intensity at 288.6 eV confirmed that there was a small amount of residual oxygenated functional groups in G/Zn<sub>0.4</sub>CdS, which was believed to be favorable for the Zn<sup>2+</sup> ions and Cd<sup>2+</sup> anchoring homogeneously onto the surface of graphene.

To characterize the microstructures of the samples SEM, TEM and HRTEM techniques have been used. Fig. 3 a presents the SEM image of G/Zn<sub>0.4</sub>CdS composites in which the width of about 100 nm is uniformly anchored on the surface of the graphene sheets. The TEM image, as shown in Fig. 3b, further confirms that nanoplates are distributed on the graphene and the corrugations of graphene sheets can be observed around these nanoplates. Fig. 3 c depicts the detailed characteristics of the nanocomposites in an enlarged TEM image in which a nanoplate with size of about 50 nm is composed of many nanocrystals. The magnified image (as arrows in Fig. 3 c) notably reveals that nanoplates are composed of many nanocrystals and the size of these nanocrystals lies mostly in the range of 10-15 nm. The lattice fringes with d spacings of 0.33 nm can be indexed to (002) crystal planes of CdS, as shown in Fig. 3 d.

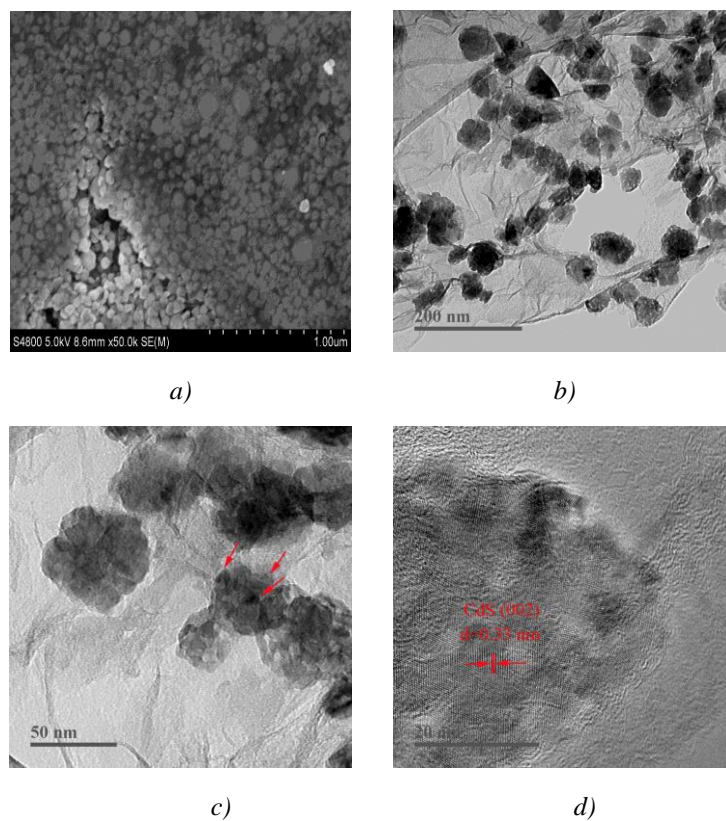


Fig. 3.  $G/Zn_{0.4}CdS$  composites images: (a) SEM, (b) TEM, (c) TEM, (d) HRTEM

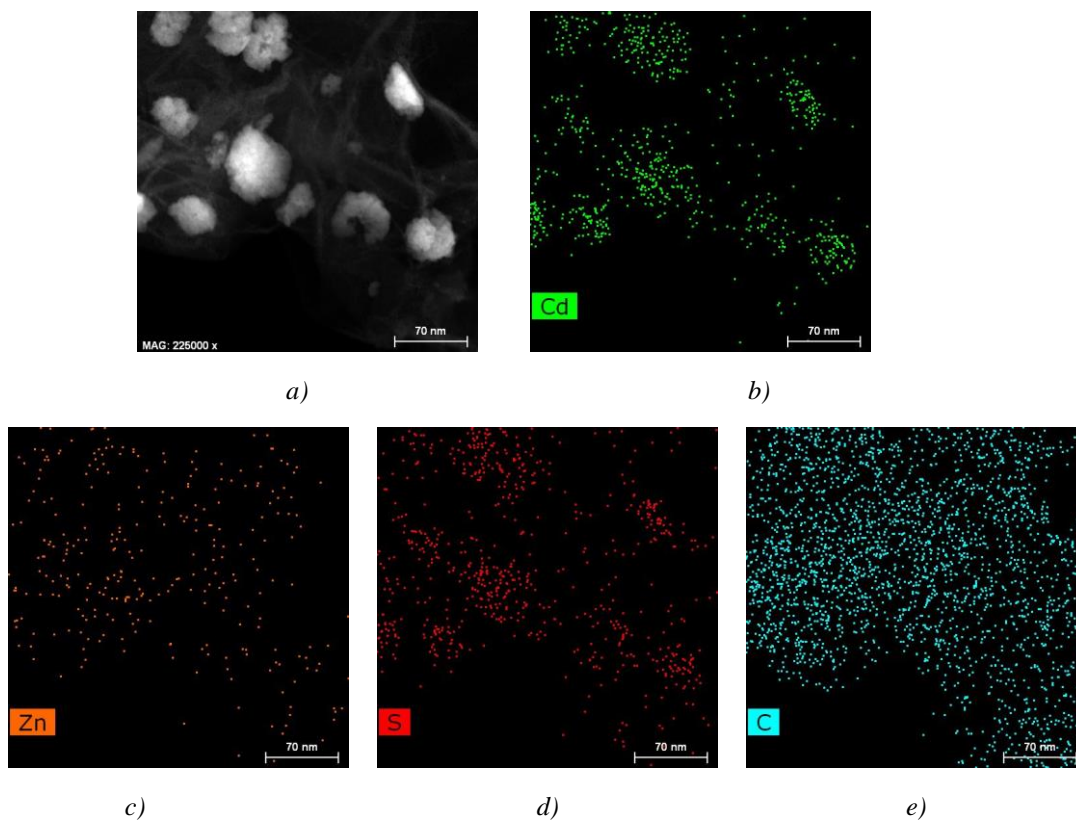


Fig. 4. EDS mapping of  $G/Zn_{0.4}CdS$  NP: (a) TEM of EDS mapping of selected area, (b) element Cd mapping, (c) element Zn mapping, (d) element S mapping, (e) element C mapping

The spatial distribution of G/Zn<sub>0.4</sub>CdS NP can further be analyzed by using the elemental mapping analysis. The TEM image shown in Fig. 4 a identified the elements of Cd, Zn, S, and C as they are in different color. The above microscopic studies provide sufficient evidence for the deposition of Zn<sub>0.4</sub>CdS NP solid solutions into graphene.

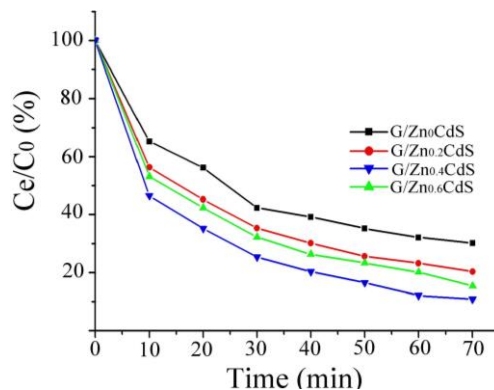
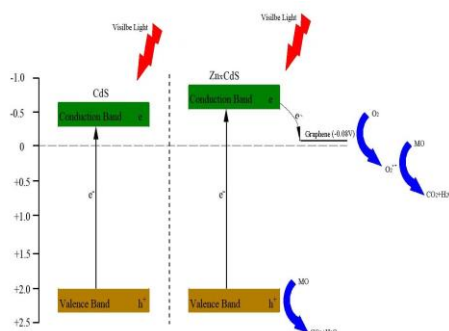


Fig. 5. Photocatalytic degradation efficiency of MO with different catalysts under visible light.

The degradation experiments were carried out to analyze the photodegradation activities of G/Zn<sub>x</sub>CdS as shown in Fig. 5. The G/Zn<sub>0</sub>CdS NP showed a limited photocatalytic activity in visible light (Only 69.9% of MO was degraded). By introducing ZnS into CdS to form G/Zn<sub>x</sub>CdS, the degradation efficiency of MO remarkably intensified with the increase of zinc content and reached to the highest photodegradation level (89.1% of MO was degraded) when  $x = 0.4$ , namely, G/Zn<sub>0.4</sub>CdS NP. The reason is that G/Zn<sub>0.4</sub>CdS NP with its proper band gap can effectively absorb the visible light and provides strong redox potential to the photoexcited electrons. However, when  $x > 0.4$ , only 84.7% of MO is degraded by G/Zn<sub>0.6</sub>CdS NP. This is attributed to the fact that by increasing the zinc content cannot efficiently absorb the visible light, thus leading to a deterioration of photocatalytic performance. Therefore, a proper band gap and an appropriate CB edge position for G/Zn<sub>x</sub>CdS are both important for achieving the excellent photocatalytic activities.



Scheme 1. Schematic illustration for the charge transfer and separation in the G/Zn<sub>x</sub>CdS NP system.

Scheme 1 illustrates the high photocatalytic activity of G/Zn<sub>x</sub>CdS NP. G/Zn<sub>x</sub>CdS nanocomposites with a suitable band gap can effectively absorb the visible light and electrons jump from the CB to the valence band (VB) by forming the photo-electrons with strong reductive ability in the CB and by leaving holes (h<sup>+</sup>) in the VB. However, the easily recombination of holes and electrons leads to a low photocatalytic activity[18]. The Zn<sub>x</sub>CdS nanoparticles are

immobilized on the graphene for which the potential of graphene/graphene•- is about -0.08 V (vs SHE, pH = 0), photo-electron can then rapidly transferred to the graphene, resulting in the electron-hole separation[19]. Finally, the photo-generated electrons transform O<sub>2</sub> (-0.28V vs. NHE) into O<sub>2</sub>•- by leaving holes (h<sup>+</sup>) in the VB. Both O<sub>2</sub>•- and holes (h<sup>+</sup>) can degrade the MO directly[20].

#### 4. Conclusions

In the present research, a novel graphene-Zn<sub>x</sub>CdS NP had been successfully synthesized via microwave method for enhancing the photocatalytic performance. Suitable band gaps have been achieved in the composites by adjusting the atomic ratio of Zn/Cd in the Cd<sub>x</sub>ZnS solid solution. By incorporating graphene into the solid solution, the synthesized G/Cd<sub>x</sub>ZnS nanoplates showed further improvement on the photodegradation of MO driven by the visible light irradiation. The synergistic effect on the photocatalytic activity was found between Zn<sub>x</sub>CdS and graphene. This work provides a promising way to couple two photocatalysts with highly efficient visible photocatalytic activity.

#### Acknowledgments

This work was supported by the Natural Science Foundation of China (NSFC, No. 50972043), the Construct Program of the Key Discipline in Hunan Province (XJF[2011] 76), the Project of Hunan Provincial Education Department (15B158).

#### References

- [1] W. Mei, M. Lin, C. S. Chen et al., *J. Nanopart. Res.* **20**(11), 286 (2018).
- [2] W. W. Yu, X. A. Chen, W. Mei et al., *Appl. Surf. Sci.* **400**, 129 (2017).
- [3] S. Y. Cao, T. G. Liu, Y. H. Tsang et al., *Appl. Surf. Sci.* **382**, 225 (2016).
- [4] W. Zhen, X. Ning, B. Yang et al., *Appl. Catal. B Environ.* **221**, 243(2018).
- [5] M. Jothibas, C. Manoharan, S. J. Jeyakumar et al., *Sol. Energy.* **159**(1), 434 (2018).
- [6] Y. C. Weng, H. Chang. *Inter. J. Hydrogen Energy.* **41**(25), 10670 (2016).
- [7] B. Zeng, X. Chen, *Dig. J Nanomater. Bios.* **11**(2), 559 (2016).
- [8] T. Su, Q. Shao, Z. Qin et al., *ACS Catal.* **8**(3), 2253 (2018).
- [9] G. Liu, C. Zhen, Y. Kang et al., *Chem. Soc. Rev.* **47**, 6410 (2018).
- [10] C. S. Chen, S. Y. Cao, H. Long et al., *J Mater. Sci.-Mater. EL.* **26**, 3385 (2015).
- [11] Y. Xiao, C. S. Chen, S. Y. Cao et al., *Ceram. Int.* **41**, 10087 (2015).
- [12] S. Lou, W. Wang, X. Jia et al., *Ceram. Int.* **42**(15), 16775 (2016).
- [13] S. Y. Cao, C. S. Chen, J. Y. Zhang et al., *Appl. Catal. B-Environ.* **176**, 500 (2015).
- [14] P. Huo, M. Zhou, Y. Tang et al., *J Alloys Comp.* **670**(15), 198 (2016).
- [15] M. Huang, J. Yu, C. Deng et al., *Appl. Surf. Sci.* **365**(1), 227 (2016).
- [16] M. Chen, P. Wu, Y. Zhu et al., *Inter. J. Hydrogen Energy* **43**(24), 10938 (2018).

- [17] W. Wan, S. Yu, F. Dong et al., *J. Mater. Chem. A* **4**, 7823 (2016).
- [18] W. K. Jo, N. C. Selvam, *Chem. Eng. J.* **371**(1), 913 (2017).
- [19] J. Zhang, J. G. Yu, M. Jaroniec et al., *Nano Lett.* **12**, 4584 (2012).
- [20] B. Zeng, W. Zeng, *Dig. J. Nanomater. Bios.* **12**(1), 215 (2017).